Effects of Porous Media on N-heptane/Air Combustion in Meso-scale Burners

Li Junwei, Wei Zhijun, Zhu Xingda, Huang Jinghuai, Yan Mi, Peng Cheng, Wang Ningfei
School of Aerospace Engineering, Beijing Institute of Technology
Beijing 100081, P.R.China

1 Introduction

Although many advances have been achieved in research on meso-scale systems in the past few years, combustion technology at small scales is still faced with some special difficulties[1], such as incomplete mixing, a large heat loss, poor combustion. Furthermore, to fulfill the promise of meso-scale power devices, high-energy-density liquid fuels are necessary. However, liquid fuels may bring additional requirements [2], such as fuel dispersion, fuel vaporization, and fuel–air mixing, all within the short flow-residence time. Ensuring the completion of these procedures before combustion is needed to minimize the emissions of soot, unburned hydrocarbons, CO, and NOx. To solve these difficulties faced by micro-combustion of liquid hydrocarbon, many measures are often used by researchers, such as, film combustion [3], electro-sprays [4], porous medium evaporator and flame holder. It can be concluded that the porous medium and heat recirculation are very good measures for liquid fuel combustion. To understand flame characteristics of liquid fuel in small tubes, meso-scale burners with porous medium were fabricated in this study. Experiments were carried out to study flame propagation and extinction in small tubes, as well as the effects of the positions of the porous media, the outer tube, and the airflow rates on the evaporation of the liquid fuel and stability of the flame.

2 Experimental setup and test combustors

The experimental system consists of an air supply system, fuel supply system, a data acquisition system and a meso-scale tube combustor with its test bench, as shown in Fig. 1. A digital syringe pump (Longer, Model LSP01-1A) and a 20ml plastic syringe are used to deliver n-heptane of 99.9% purity into the combustor through a stainless steel capillary tube(ID 0.26 mm, OD 0.4mm). An electric mass flow controller (Sevenstar, Model D0727A/ZM 0–5SLM) precisely controls and monitors the mass flow rates of air within ±2% accuracy of the full scale. Wall temperatures of the micro-combustor are measured using K-type thermocouples. These measured temperatures have a standard error less than ±0.15% (400–1300 °C). All experimental results are obtained after the combustors reach steady states. The surface temperatures of the outer tube are also measured using an infrared thermal imager (FLIR, Model A40). Shapes and movement of the flame are recorded by a high-definition camcorder.

The schematic diagram of a tube combustor is shown in Fig. 2. It consists of a small quartz inner tube(IT), a piece of porous media (PM), a quartz outer tube (OT) and a stainless steel capillary tube.

Correspondence to: correspondence author email address here

The inner tube has a length, inner diameter, and outer diameter of 100, 4, and 6 mm, respectively. The IT is mounted horizontally on a stainless steel tee joint, with one end open to the atmosphere. The PM (10mm long) is inserted into the IT. To enhance vaporization of liquid heptane, one end of the capillary tube is inserted into the PM. The OT is coaxially placed outside the IT to recover the exhaust heat. Pressurized air is regulated to one atmosphere and enters the IT along the axis. Polyacrylonitrile-based graphite felt, with a porosity of 87%, is used as the porous media, as shown in Fig. 3. The graphite felt is composed of a lot of micron filaments of a diameter 20 and is used as an evaporator in this study. When the PM is heated by the flame or the tube wall, vaporization of heptane is enhanced. Meanwhile, microchannels in the PM also enhance mixing of air and fuel vapor. In this study, the right end of the IT is considered as an original point and marked as ‘‘O’’. X-axis is set on the axis of the IT and Y-axis is the transverse direction. To understand effects of the PM on flame stability, ModelB and ModelC are designed. In ModelB, the PM is placed upstream of the tip of the capillary tube and its right surface is 58.5mm from the IT exit, whil in ModelC the tip of the capillary tube is inserted into the PM.

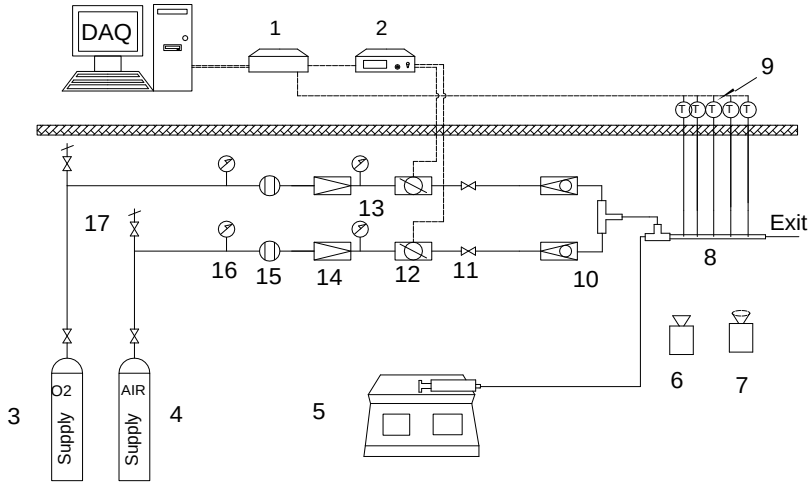

1.DAQ 2. Mass flow controller 3.Oxygen tank 4.Air tank
5. Syringe pump 6. CCD 7. IR imager 8.Micro-combustor
9.Thermocouples 10. Check valve 11. Hand valve 12. Flow control valve
13&16. Pressure gage 17. Relief valve

Fig. 1 Schematic of the experimental setup

Six shielded K-type thermocouples with 0.5mm diameter are used to measure the surface temperature on the combustors. TC3, TC4, TC1 and TC5 are tied on the outside wall of the IT along the axis. TC6 is a shielded K-type thermocouple with 1mm diameter, which is placed at the exit of the IT to measure the exhaust temperature. TC2 and the capillary tube are inserted into the PM to measure its temperature. TC7 is tied on the outside wall of the OT.

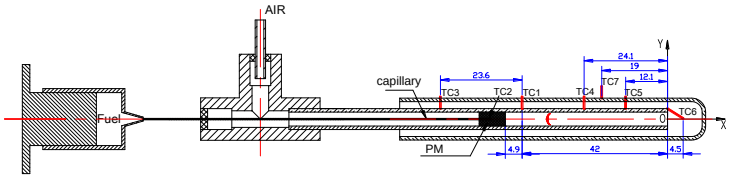

Fig. 2 Schematic of the test combustor ModelC

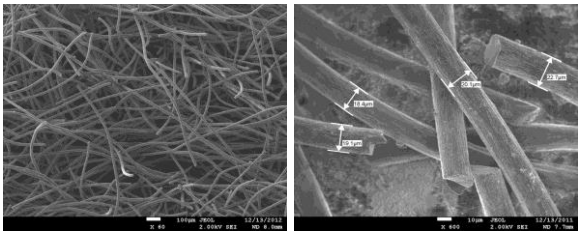

Fig. 3 Photographs of the porous media used in experiments

4 Mathematical model

Combustion in the test combustors is simulated using a commercially available CFD code, FLUENT 6.2, results from which are analyzed along with those of experimental tests to effectively design microburners. Mathematical model includes energy conservation equations for solid and gas phases, mass conservation equation for reactants, continuity equation for mixture, momentum equation and the ideal-gas state equation. To consider the effects of gas radiation on wall temperature, DO(Discrete Ordinate) radiation model is adopted in consideration of the gas phase as a gray absorbing emitting medium. Furthermore, the Discrete Phase Model (DPM) based on the Euler-Lagrange method is employed to simulate atomization of n-heptane and droplet's movement. To predict droplet vaporization, a simple vaporization and heating model is employed in this study. When the temperature of a droplet reaches the vaporization temperature, the droplet proceeds to evaporate and obey laws of the mass-transfer. Multicomponent diffusion, thermal diffusion, variable thermo-chemical properties, and variable transport properties are considered. The governing equations are discretized and simultaneously solved by the finite volume method. The number of grids is determined through the grid-independence test.

Applied boundary conditions are as follows: no-slip conditions and dXi/dr = 0 on the inside wall of the combustor, ambient air with varied heat transfer coefficient on the outside wall of the burners. Constant emissivity of 0.72 is applied to the quartz tube, which is obtained from the infrared images calibrated using the thermocouple TC7. Numerical simulations were conducted for the same conditions as those for experiments. In the simulations, the flame was ignited by specifying a high temperature wall (~1500 K). Convergence tests showed that the results of calculations with error tolerance 0.01 and 0.001 are qualitatively the same and quantity difference is less than 3%.

3 Results and Discussion

3.1 Numerical Validation: Flame-stabilization phenomenon in ModelC

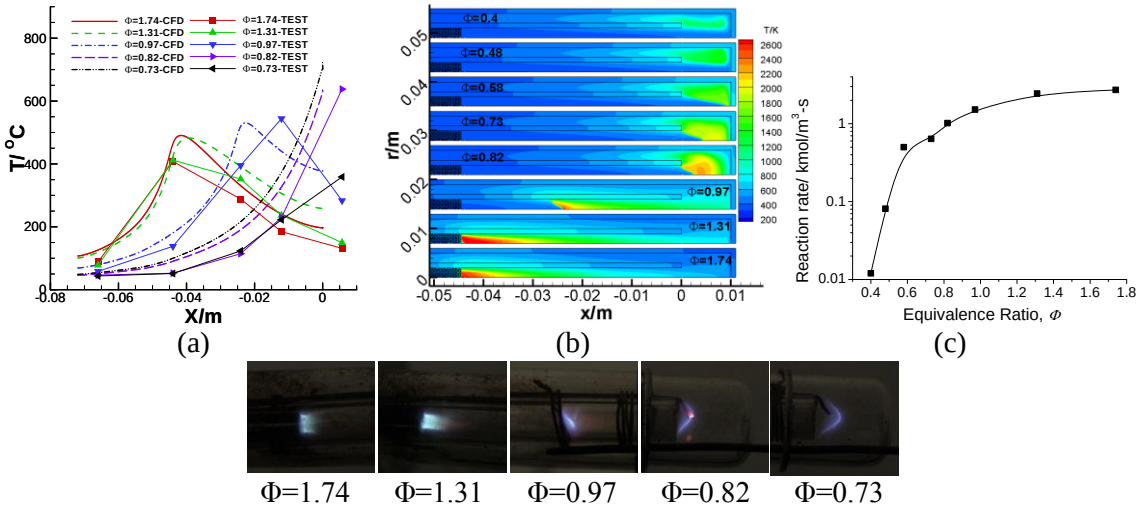

Fig. 4 Combustion of n-heptane/air in ModelC at Q_f =0.34mg/s. (a)Comparison of measured and predicted wall temperature of the IT; (b)predicted temperature fields; (c)one-step reaction rate; (d)flame photos at different equivalence ratios

To validate the numerical model and understand heptanes flame propagation features in a micro-tube combustor, ModelC is simulated using the above method under the experimental conditions. Fig. 4(a) shows the temperature distributions along the IT surface in ModelC. Compared with the measured temperature, the predicted temperatures are a little higher. However, the quantitative difference is less than 18%, which is usually acceptable for most computational predictions. Predicted temperature fields in ModelC are shown in Fig. 4(b). It indicates that at Q_f =0.34mg/s, with the decrease of equivalence ratio, the flame moves from inside to outside the IT and gases temperature decreases gradually. Fig. 4(d) shows that when Φ=1.74, the flame adheres to the PM and is shorter than that at Φ=1.31. When Φ is decreased to 0.97, the flame stays in the middle of the IT. Furthermore, when Φ<=0.82, the flame stabilizes at the exit of the IT. All these phenomena are correctly predicted by the simulation. Additionally, predicted reaction rate as a function of Φ is plotted in Fig. 4(c). It indicates that when Φ< 0.73, the chemical reaction rate falls down rapidly and flame stability becomes worsen, which agrees well with the measured fuel-lean limit, Φ=0.73. All above observations justify the present approach to micro-combustor design combining measurements with computations.

3.2 Droplet combustion in a combustor without PM

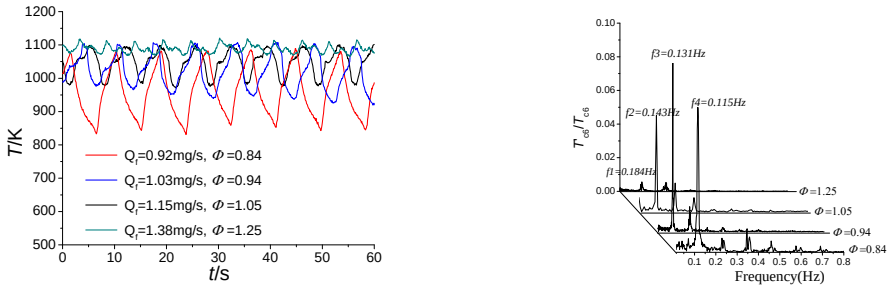

(a) TC6 variation with time (b)TC6 amplitude versus frequency

Fig. 5 Gas temperature(TC6) fluctuation with time in ModelB at V_a =1.1m/s

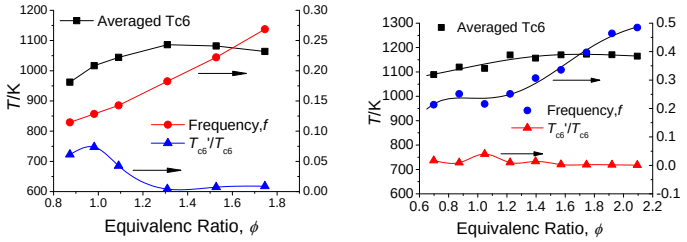

(a) V_a =1.1m/s (b) V_a =1.3m/s

Fig. 6 Measured peak temperatures, averaged temperatures of TC6 and frequencies of TC6 fluctuation at different equivalence ratios

In experiments, it was found that if there is no porous media in ModelC, discontinuous fuel droplets are formed at the exit of the capillary tube. Such discontinuous fuel injection results in an unstable flame and leads to extinguishment. To understand effects of discontinuous fuel injection on combustion stability, experiments in ModelB were conducted at air flow velocity V_a =1.1m/s. TC6 temperature oscillations with time are plotted in Fig. 5(a). The figure shows that with the increase of Φ, amplitude of the TC6 fluctuations decreases gradually. At Φ=0.87, the amplitude is about 220K, while at Φ=1.31, the amplitude is reduced to 50K. The reason may be that for a fixed air flow rate, a large equivalence ratio leads to an increased heptane flow rate. At a smaller equivalence ratio, the size of a droplet slowly becomes larger, resulting in a lower evaporation rate. But once the droplet drops on the IT wall, the hot wall dramatically increases the evaporation rate and local equivalence ratio is greatly changed, which leads to a dramatic temperature change. In contrast, at a large heptane flow rate, the fuel injection rate is larger than the evaporation rate and excess fuel drops on the wall. Therefore, there always is a fuel film on the wall, which reduces the gas temperature fluctuation. To further investigate the signals, spectral graphs were generated, using the FFT algorithm. The spectral graphs in Fig. 5 (b) indicates that several frequencies existed in the traces and the strongest peak occurred at different frequencies at different Φs. Furthermore, as Φ increases, the frequency corresponding to the strongest peak increases because of a larger fuel flow rate.

To understand effects of incoming air velocity on the flame oscillating, averaged gas temperature and frequency were calculated using the experimental data. The averaged temperature of TC6 in Fig. 6 indicates that as the equivalence ratio increases, the gas temperature gradually increases and reaches its maximum value at Φ= 1.4. This is the result that for the same air flow rate, the increased equivalence ratio enlarges the fuel flow rate and hence the flame is blown to the bottom of the OT, which leads to increased TC6 temperature. Furthermore, Fig. 6 shows that frequency of the TC6 oscillation becomes larger as Φ increases. Since at a small Φ, a droplet needs a long time to form and drop from the tip of the capillary tube, the frequency is very small. While at a larger Φ, a larger fuel flow rate reduces the time to form and drop a droplet, and hence the frequency becomes higher. In addition, Fig. 6 indicates that the amplitude of TC6 fluctuation first increases and then decreases, and the maximum amplitude occur at Φ= 1. This is because at a small Φ, any small change in heptane droplets can drastically affect

the flame, causing significant changes of TC6. When Φ is relatively large, a lot of liquid heptane accumulates on the IT wall, and forming and falling down of heptane droplets do not cause a drastic change of the flame. Therefore, TC6 amplitude is close to zero.

3.2 Droplet combustion in a combustor with PM

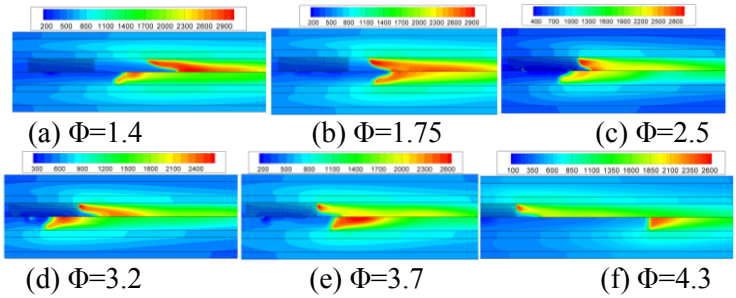

(a) Φ=1.4 (b) Φ=1.75 (c) Φ=2.5

(d) Φ=3.2 (e) Φ=3.7 (f) Φ=4.3

Fig. 7 Predicted temperature fields in ModelC and ModelB at Q_f =0.92 mg/s. (In each picture, the upper part is the temperature in ModelC, the lower part is the temperature in ModelB)

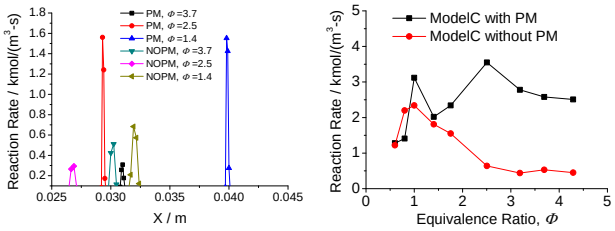

(a)Reaction rate on the axis of the IT (b)Maximum reaction rate at different Φ

Fig. 8 Comparison of predicted one-step reaction rate of n-heptane/air in ModelC and ModelB at Q_f =0.92 mg/s

To investigate influence of porous media on flame position and reaction rate, numerical simulations were conducted in ModelC and ModelB. Flames in Fig. 7 indicate that in ModelC when Φ>2.5, the flame always stays on the PM surface with a shape of cone. While for ModelB, the flame stays at different places in the IT at different Φ. Furthermore, Φ does not greatly change the flame shapes in ModelC due to the flame stabilization on the PM. However, in ModelB, the flame shows various shapes and moves back and forth at different Φ, which suggests that such change reduces the flame stability, making it unstable and even causing extinguishment. Furthermore, it can be seen from the figures that porous media enhances mixing of heptane and air, which increases the flame temperature in ModelC, and makes the flame front much thinner, reaction intensified.

Predicted reaction rates of n-heptane/air in Fig. 8(a) indicate that except Φ=3.7, the reaction rate in ModelC is 3-5 times larger than that in ModelB. This could be duo to that at Φ=3.7, the fuel flow rate is large and the reaction zone stays at the downstream of the outer ring of the PM, as shown in Fig. 7(e), which leads to low reaction rate on the IT axis. Furthermore, Fig. 8(b) shows that at fuel-rich condition (Φ>1), the maximum reaction rate at each Φ in ModelC is greater than that in ModelB. Because when Φ=2.5, the flame still stays on the surface of the PM, the largest reaction rate within the equivalence ratio range is reached in ModelC. At Φ<2.5, as Φ decreases, the flame moves away from the PM and the reaction rate declines slowly. At Φ=1.4, the lowest reaction rate is reached in ModelC. Subsequently, due to enhanced mixing of heptanes/air, the reaction rate increases again in ModelC, reaching a peak value at Φ=1. In contrast, in ModelB, Fig. 8(b) indicates that as Φ decreases, the reaction rate is gradually increasing, reaching the maximum value at Φ=1. This is due to that as Φ decreases, the flame is moving towards the IT exit, and fuel vapor mixes and reacts more completely with air. At Φ=1, their reaction rate reaches a maximum and then declines.

4 Conclusion

Two meso-scale burners were designed and tested in this study. The extinction characteristics of the burners and temperature distributions of the burners were systematically studied. Some of the salient findings from the study are as follows:

1) If there is no porous media in the burner, flame oscillation will occur and the flame is vulnerable to external factors, and finally extinguished. At the same air flow rate, with the increase of equivalence rate, the amplitude of flame temperature oscillations monotonically decreases and the oscillating frequency increases.
2) The porous media in the burners play an important role in the flame stabilization. When porous media is added, flame oscillation disappears. At low airflow rates, the flame is stabilized on the PM surface. With an increase in the airflow rate, the flame is gradually blown toward the inner tube exit, eventually being blown out of it.

References

[1] Ju Y. and Maruta K. (2005). Microscale Combustion: Technology, Development and Fundamental Research. Prog. Energy Comb. Sci. 37:669.

[2] Mujeebu M.A, Abdullah M.Z, Abu Bakar M.Z., Mohamad A.A., Abdullah M. K. (2009). A Review of Investigations on Liquid Fuel Combustion in Porous inert media. Prog. Energy Comb. Sci. 35:216.

[3] Pham T.K., Dunn-Rankin D., Sirignano W.A.(2007). Flame structure in small-scale liquid film combustor. Proc. Combust. Inst. 31: 3269.

[4] Kyritsis D.C., Coriton B., Faure F., Roychoudhury S., Gomez A. (2004). Optimization of a Catalytic Combustor Using Electrosprayed Liquid Hydrocarbons for Mesoscale Power Generation. Combust. Flame, 139: 77-89.